

# FGGM: Formal Grey-box Gradient Method for Attacking DRL-based MU-MIMO Scheduler

Thanh Le<sup>1,2</sup>, Hai Duong<sup>3</sup>, Yusheng Ji<sup>2,1</sup>, ThanhVu Nguyen<sup>3</sup> and John C.S. Lui<sup>4</sup>

<sup>1</sup>The Graduate University for Advanced Studies (SOKENDAI), Japan

<sup>2</sup>National Institute of Informatics (NII), Japan

<sup>3</sup>George Mason University, USA

<sup>4</sup>The Chinese University of Hong Kong, China

**Abstract**—In 5G mobile communication systems, multi-user multiple-input multiple-output (MU-MIMO) has been applied as a core technology to enhance spectral efficiency and support high data rates for accommodating multiple users. To fully exploit the spatial diversity and maximize spectral efficiency while providing fairness among users, the base station (BS) needs to select a subset of users for data transmission. Given that this problem is NP-hard, deep reinforcement learning (DRL)-based methods have been proposed to infer the near-optimal solutions in real-time [1]. However, this approach has an “*intrinsic security problem*”. This paper investigates how a group of adversarial users can exploit unsanitized raw CSIs to launch a throughput degradation attack. We assume that the group of adversarial users have obtained the DRL policy. Most existing studies only focused on systems in which adversarial users can obtain the exact values of victims’ CSIs, but this is impractical in the case of uplink transmission in LTE/5G mobile systems. We note that the DRL policy contains an observation normalizer which has the mean and variance of the observation to improve training convergence. Adversarial users can then estimate the upper and lower bounds of the local observations including the CSIs of victims based solely on that observation normalizer. We develop an attacking scheme Formal Greybox Gradient Method (FGGM) by leveraging polytope abstract domains, a technique used to bound the outputs of a neural network given the input ranges. Our goal is to find one set of intentionally manipulated CSIs which can achieve the attacking goals for the whole range of local observations of victims. Experimental results demonstrate that FGGM can determine a set of adversarial CSI vector controlled by adversarial users, then reuse those CSIs throughout the simulation to reduce the network throughput of a victim up to 70% without knowing the exact value of victims’ local observations. This study serves as a case study and can be applied to many other DRL-based problems, such as a knapsack-oriented resource allocation problems.

**Index Terms**—deep reinforcement learning, neural networks verification, adversarial attack, multi-user massive MIMO

## I. INTRODUCTION

Massive multiple-user multiple-input multiple-output (MU-MIMO) is a core technology that can greatly enhance the efficiency of current access networks by using numerous antennas at the base station [2]. This allows the base station to perform multi-user beamforming and to serve many user in the same time-frequency resource block. However, in dense environments where users are closely located, significant inter-user interference can occur. This issue can be mitigated by selecting only a group of users that contribute to the highest overall spectral efficiency and fairness [3, 4].

Since channel state information (CSI) between users and base station change rapidly in mobile networks where users move frequently, as a result, base station must resolve the fair resource scheduling problem while maximizing spectral efficiency in real-time [5, 6]. However, the fair scheduling problem can be reformulated as an integer linear programming (ILP) problem and is NP-hard [4]. The complexity of solving ILP makes it challenging to design optimal yet fast schedulers for next-generation access networks, especially with a large number of users and resource blocks. Recent studies applied deep reinforcement learning (DRL) to find near-optimal solutions for NP-hard problems such as travelling salesman problem (TSP) or knapsack problems [7]. In [1], DRL-based MU-MIMO schedulers were trained and tested on realistic channel models and real-world channel measurements, and demonstrated a close performance to the optimal proportional fairness ( $\text{OptPF}$ ) scheduler in terms of spectral efficiency and fairness. Especially, the DRL-based scheduler has a small computational complexity, so it can solve the problem in network scenarios where  $\text{OptPF}$  is computationally infeasible.

Nevertheless, the MU-MIMO scheduler based on DRL introduces an “*intrinsic security problem*” as it utilizes the unsanitized CSI from users to make scheduling decisions. DRL is known to be susceptible to adversarial observations crafted by attackers to manipulate the decisions of DRL agents, which can significantly degrade the performance of a well-trained DRL policy [8]. Given that the reported CSIs form part of the inputs/observations for the DRL-based scheduling policy, a few adversarial users can falsify their CSIs to negatively influence user selection outcomes such as to degrade the throughput of normal users, e.g., victims.

In this work, we investigate how to craft the most detrimental adversarial CSIs, which are determined by the trained DRL policy and the CSIs of victims. We propose a threat model in which adversaries know the trained DRL policy for white-box testing, as it can generate better adversarial examples compared to black-box testing. This represents the worst-case scenario that network operators need to prepare for. If the DRL-based scheduler can survive this scenario, it would have a better chance of being robust against attacks that are agnostic to DRL policies.

Most prior works on attacking MU-MIMO resource allocation algorithms relied on precise knowledge of victims’

CSI, which adversarial users can capture by listening to the plain text CSI feedback to the base station [9, 10]. This approach might be impractical for systems with uplink CSI reference signal, where the base station estimates CSI instead of relying on users feedback, or for systems with physical layer encryption of CSI feedback. On the other hand, our proposed threat model assumes that the adversaries work for all potential values within the normal ranges of victim observations including the victim CSIs. The total domain of the observation space is established by concatenating the adversarial users' concrete observations with the lower and upper bounds of the victims' observations. Our conceptual contribution is the grey-box threat model for DRL-based MU-MIMO scheduler, which incorporates both white-box (DRL policy) and black-box testing elements (victims' observations).

We then propose the Formal Greybox Gradient Method (FGGM) to solve for the adversarial CSI under our grey-box threat model. FGGM leverages the polytope abstraction domain [11], which is commonly used in deep neural network (DNN) verification [12, 13], to handle the observation intervals. FGGM subsequently propagates these observation boundaries through the hidden and output layers of the DRL policy to construct an objective function on the output bounds. Note that the upper bounds of the output determine the chance that base station select an user, i.e. the highest possible performance when base station selecting that user. We formulate the problem of finding adversarial CSIs such that the upper bounds for all outputs that allow victims to transmit data are minimized for all possible victim CSIs. Thus, this attack strategy provides "a single adversarial input" at the initiation of the attack, without the need of recalculating during the attack. Given that the abstract domain is differentiable, we solve this problem using stochastic gradient descent.

To this end, this paper introduces a new and practical adversarial attack strategy for DRL-based massive MU-MIMO schedulers. The key contributions of this paper are:

- 1) Develop a grey-box threat model for DRL-based MU-MIMO schedulers, which encompasses the trained DRL model and possible ranges of victims' observations.
- 2) Propose FGGM to solve for adversaries' observations that degrade victim throughput for all victim observations.
- 3) Demonstrate that FGGM outperforms black-box or sampling-based white-box attacks via projected gradient descent (PGD) in reducing access probability and degrading throughput across various widths of input bounds and search spaces.
- 4) A single attacker can degrade victim throughput by up to 9.5%. When 50% of users are attackers, the victim's throughput can be drastically reduced by up to 70%.
- 5) The implementation of FGGM is publicly available at (redacted).

This paper is organized as follows. Section §II presents the target DRL-based MU-MIMO scheduler and gives a primal on DNN verification. Section §III explains grey-box threat model, which envisions the capabilities and limitations of the

attackers. We describe our proposed FGGM attack in Section §IV, followed by the evaluation and discussion section.

## II. PRELIMINARIES

In this section, we briefly describe the target MU-MIMO network model, explain why MU-MIMO scheduling is a difficult problem, and how it was addressed by using DRL. We then describe how DRL-based schedulers which can infer the near-optimal solution for this problem in real-time.

### A. Network Models

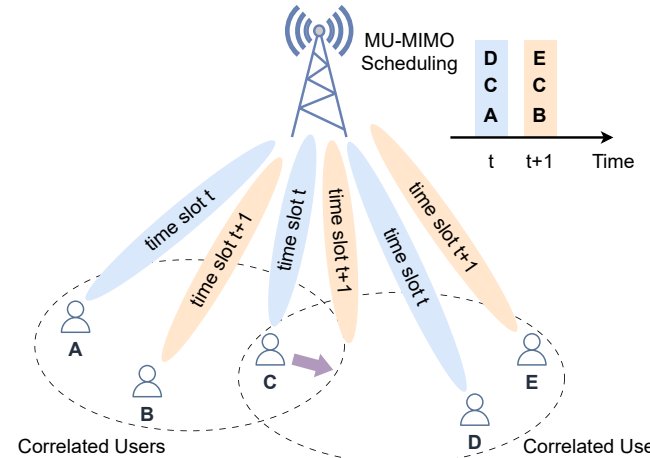


Fig. 1: The system model of the MU-MIMO scheduling problem.

Consider a single-cell wireless network base station with  $M$  multiple-input multiple-output (MIMO) antennas (Fig. 1). The base station uses the orthogonal frequency division multiplexing (OFDM) technique with  $B$  orthogonal resource blocks, and performs MU-MIMO transmission in a time-slotted manner. Each resource block is shared among  $L$  single-antenna mobile user. Assume that the time division duplexing (TDD) mode is used, where  $L$  users periodically send orthogonal pilot sequences to the base station for channel estimation, and CSI remains constant during a time slot. The MU-MIMO scheduler then obtains the full knowledge of CSI of  $L$  associated users. Using the full CSI matrix, base station selects a set of  $N \leq \min(\bar{N}, L)$  among  $L$  users to transmit data (either uplink or downlink), where  $\bar{N}$  is the maximum number of users that can be selected in one resource block and one time-slot.

When considering an uplink transmission, base station will receive:

$$\mathbf{y} = \mathbf{H}\mathbf{u} + \mathbf{n}, \quad (1)$$

where  $\mathbf{u} \in \mathcal{C}^N$  are transmitted symbols,  $\mathbf{H} \in \mathcal{C}^{M \times L}$  is the CSI matrix,  $\mathbf{n} \sim \mathcal{CN}(0, \sigma^2 \mathbf{I})$  is an additive white Gaussian noise with the variance  $\sigma^2$ , and finally,  $\mathbf{y} \in \mathcal{C}^M$  is the received signal vector at the base station. Next, base station calculates the zero forcing beamformer using the estimated CSI matrix  $\hat{\mathbf{H}}$  as:

$$\mathbf{W} = \hat{\mathbf{H}}(\hat{\mathbf{H}}^H \hat{\mathbf{H}})^{-1}. \quad (2)$$

After receiving the signal  $\mathbf{y}$ , base station decodes the transmitted symbols  $\mathbf{u}$  via:

$$\hat{\mathbf{u}} = \mathbf{W}^H \mathbf{y}. \quad (3)$$

Then, instantaneous transmission rate achieved by each user  $l \in \{1, \dots, L\}$  in resource block  $b \in \{1, \dots, B\}$  and time slot  $t \in \{1, \dots, T\}$  is calculated as:

$$r_{l,b}^t = \log(1 + \text{SINR}_{l,b}^t), \quad (4)$$

where  $\text{SINR}_{l,b}^t$  is the received signal to interference-plus-noise ratio (SINR) at base station from each selected user  $l$  at resource block  $b$  and time slot  $t$ .

### B. MU-MIMO Scheduling Problem

Base station needs to select  $N$  users among total  $L$  users to maximize the throughput while ensuring fairness. Let  $r_l^t$  be the instantaneous rate user  $l$  scheduled with other users. Also, let  $R_l^t$  represent the average transmission rate that has been allocated to user  $l$  up to time slot  $t$ , then we have:

$$R_l^{t+1} = (1 - \beta)r_l^t + \beta R_l^t \quad (5)$$

where  $x_l^t$  is the binary decision variable representing whether user  $l$  is selected for transmission time slot  $t$ , and  $\beta \in [0, 1]$  is the weight to control the importance of instantaneous rate in comparison to the average allocated transmission rate. At each time slot  $t$ , base station solves the following  $\text{Opt}_{\text{PF}}$  problem as follows:

$$\begin{aligned} & \underset{x_l^t, \forall l \in \{1, \dots, L\}}{\text{maximize}} && \sum_{l=1}^L \frac{r_l^t x_l^t}{R_l^t}, \\ & \text{subject to} && \sum_{l=1}^L x_l^t \leq \bar{N}, \end{aligned} \quad (6)$$

where  $x_l^t \in \{0, 1\}$ . This scheduling problem can be reformulated as an ILP problem, which is NP-hard [4]. To solve this NP-hard combinatorial optimization problem, previous works trained DRL agents to infer the near-optimal solution from the problem statement in real-time [1].

### C. DRL-based MU-MIMO Scheduler

To solve this difficult problem in real-time, we consider a recent open-source DRL-based beam allocation algorithm [1] using soft actor critic (SAC) and  $k$  nearest neighbor (KNN). First, this method reformulates the combinatorial optimization problem into the following Markov decision process (MDP):

1) *Observation Space*: Let  $o_l^t := [\gamma_l^t, R_l^t, h_l^t]$  be the observation for each user  $l, \forall l \in \{1, \dots, L\}$ , where  $\gamma_l^t = \frac{r_l^t}{\bar{r}_l^t}$  is the normalized instantaneous rate, and  $\bar{r}_l^t$  is the maximum rate of user  $l$  when only  $l$  transmits data.  $R_l^t$  is the average allocated transmission rate till time  $t$  for user  $l$ , and  $h_l^t$  is the CSI of user  $l$  at time  $t$ .

2) *Action Space*: The action  $a^t$  is an integer, which indicates the index to the set of users. It takes the value from the action set  $\mathcal{A} = \{1, 2, \dots, \sum_{i=1}^N \binom{L}{i}\}$ . We can decode  $a^t$  as a binary variable  $x_l^t$ , which contains the decision whether the base station select user  $l$  to transmit at time slot  $t$  or not.

3) *Action Generation*: The policy network  $\pi(\cdot|o^t; \theta_\pi)$  takes the observation  $o^t$  as the input to generate the action  $a^t$ . To design the policy network, a naive approach is to design the policy network with an output size of  $|\mathcal{A}|$ , where  $a^t$  represents the index of the maximum output unit of the policy network. However, this approach becomes impractical as the size of the search space  $\mathcal{A}$  grows. In [1], the Wolpertinger architecture [14] is implemented to select actions from a large discrete action space. The policy network  $\pi(\cdot|o^t; \theta_\pi)$  maps observations to a ‘‘proto action’’  $u^t \in [0, 1]^D$  rather than directly mapping the observation space to the large discrete action space, where  $D$  is the number of dimension for proto action. When  $D$  increases, the number of discrete actions per dimension of  $u^t$  decreases, which improves the precision of the mapping from continuous proto action  $u^t$  to discrete action  $a^t$ . This proto action serves as a continuous representation of large discrete action space  $\mathcal{A}$ , requiring only  $D$  continuous outputs from the policy network instead of  $|\mathcal{A}|$  output units. Discrete actions  $a^t$  are then placed in the continuous proto-action space in an equal distance. For example, if there are  $\sum_{i=1}^N \binom{L}{i}$  discrete actions and the proto action space has  $D$  dimensions, then each dimension of the proto action space will be divided in to  $\sqrt[D]{\sum_{i=1}^N \binom{L}{i}}$  equidistant points. Then, each combination of points in all  $D$  dimensions represents a discrete action. The policy network  $\pi(\cdot|o^t; \theta_\pi)$  takes the observation  $o^t$  as an input and outputs  $\hat{u}^t$  as the predicted proto action. The corresponding discrete action is one among  $k$ -nearest neighbor of  $\hat{u}^t$  in the proto action space.

4) *Action Refinement*: The critic network  $Q(o^t, u^t; \theta_Q)$  chooses the best among the  $k$  nearest discrete actions from the generated proto action. For example, the nearest proto action from the inferred proto action may have a low  $Q$ -value, while others in the set of  $k$ -nearest neighbors may all give high  $Q$ -values. To avoid picking outlier actions, the critic network  $Q(o^t, u^t; \theta_Q)$  is used to evaluate the  $Q$ -value of  $k$ -nearest neighbors from the inferred proto action  $\hat{u}^t$ . The critic network in this Wolpertinger architecture takes the observation and the proto action as the input and produces the estimated  $Q$ -value. Finally, the discrete action that maximizes the  $Q$ -value among the  $k$ -nearest neighbors will be chosen. Note that SAC is the training algorithm for actor and critic in this architecture [15].

5) *Reward*: The reward for the centralized DRL-based scheduler at the base station is defined for each time slot  $t$ :

$$r^t = \sum_{l=1}^L \frac{r_l^t x_l^t}{R_l^t}, \quad (7)$$

$r_l^t$  is the instantaneous rate of the  $l^{\text{th}}$  user time slot  $t$ ,  $R_l^t$  is its cumulative amount of transmitted data at  $t$ . By training via this reward function, the DRL-based scheduler to choose users to maximize the instantaneous rate for users having low cumulative rates, which also provides quality solutions for Problem 6.

#### D. Formal Verification of DNN - A Primal

DNN, just like traditional software, can have “bugs”, e.g., producing unexpected results on inputs that are different from those in training data, or small perturbations to the inputs can result in misclassification. To address this question, researchers have developed various algorithmic techniques and supporting tools to verify properties of DNNs [16, 11, 13, 17, 18, 19, 20, 21].

There are three main approaches to solve the DNN verification problem: (1) constraint-based approaches, (2) abstraction-based approaches, and (3) hybrid approaches. Obtaining the exact solution for constraint-based approaches can be time consuming when the size of the given DNN increases [16]. Alternatively, abstraction-based techniques and tools use abstract domains, such as polytope (e.g., DeepPoly [11]), to scale up verification while slightly reduce the accuracy. Abstract domains such as interval, zonotope, or polytope over-approximate output values of nonlinear units of DNNs. The main objective of the abstraction is to construct polyhedral over-approximations defined by linear inequalities that tightly enclose the possible outputs of the non-linear functions, e.g., rectified linear unit (ReLU). NeuralSAT [13, 17] combined constraint-based verification and abstraction-based techniques to handle more challenging properties and further increase the size of verifiable DNN.

In addition, abstraction-based verifiers are integrated in supervised training of DNN models, such that the result models is easier to verified it robustness properties [22]. However, DNN verification have not been applied widely to aid the attack the DRL-based system. To the best of our knowledge, we are the first to leverage DNN verification to generate adversarial observations for DRL.

### III. THREAT MODEL

This section envisions potential threats for the considered DRL-based MU-MIMO scheduling system (see Fig. 2). We will explain realistic assumptions on the capabilities and limitations of the adversarial users.

#### A. The Interactions of Adversaries

In our proposed grey-box threat model (Fig. 2), there exists  $L_{adv}$  adversarial users and  $L_{vic}$  victim such that  $L = L_{adv} + L_{vic}$ . A designated cluster (i.e, one among the attackers) head controls all adversarial users. This cluster head obtains the model of a DRL agent to compute adversarial CSI values for users under its control so to disrupt network performance for the victims. To facilitate the computation of adversarial observations, the cluster head must possess the sufficient computational capability, or it can offload this task to a cloud server. Once the adversarial CSI values are calculated, the cluster head distributes this information to  $L_{adv} - 1$  other adversarial users. Subsequently, the adversarial users are tasked with either reporting the falsified CSI to the base station or adjusting the CSI reference signal such that the base station receives the adversarial CSI calculated by the cluster head. Note that this attack strategy provides a single

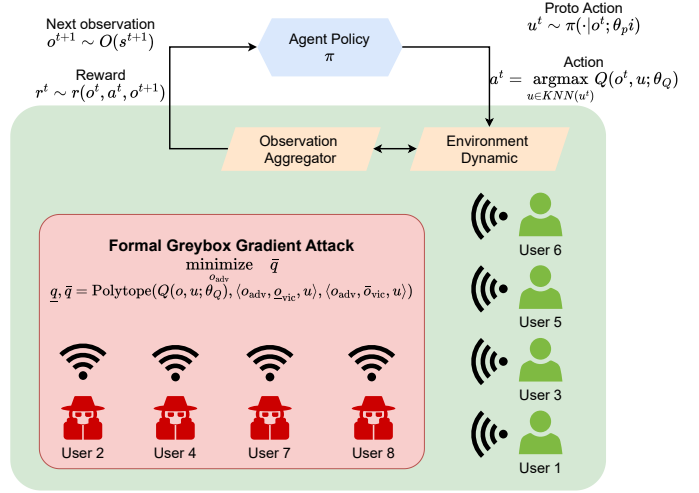


Fig. 2: Threat model of DRL-based scheduler for MU-MIMO networks.

adversarial input at the initiation of the attack, without the need of recalculating during the attack. As FGGM computes the adversarial CSI for potential victim CSIs within their normal ranges, the attack remains effective even if the victim CSIs change due to movement.

#### B. Victim’s Observation

To search for an adversarial input, attackers need to estimate the CSI values of target users. Prior works have primarily focused on scenarios where attackers know the exact CSI values of victims [9, 10]. This line of work typically involves downlink data transmission, where the base station broadcasts a CSI reference signal to users. users then estimate the CSI and provide feedback to the base station in plain text, which can potentially be intercepted by adversaries. One approach to mitigate this drawback is to encrypt the CSI feedback at the physical layer to maintain confidentiality from malicious users. Obtaining the exact values of victim CSI is more challenging in the context of uplink transmission in LTE/5G mobile systems, where users send the CSI reference signal to the base station. Since attackers are located in different locations than the base station, the CSI reference signals they measure will differ from the CSI measured at the location of the base station.

In this work, our method estimates the boundaries of victim observations by leveraging the observation normalizer, which is an essential component of a DRL agent, aiding in stabilizing the training process [23]. Given that DRL observations often consist of multiple dimensions, each dimension bounded by an interval, the observation normalizer transforms each dimension to follow a standard Normal distribution. This normalization process is similar to data whitening in regression tasks to ensure that all components of the observations have an equal influence. Without the observation normalizer, training DRL algorithms for most continuous control tasks becomes impractical. The observation normalizer contains the mean

and standard deviation of observations obtained during the training phase. Hence, these statistics can be leveraged to estimate the average observation values of a typical user. Let  $\mu_o$  and  $\sigma_o$  denote the mean and standard deviation of the observation vector for a user, which can be extracted from the observation normalizer of the trained SAC agent. We can bound the victim's observations between  $\mu_o \pm \delta_o \sigma_o$ , where  $\delta_o$  is a scaling factor controlling the width of the bounds. Similarly, the search space for potential attackers can be defined within the same limits.

#### IV. FORMAL GREY-BOX GRADIENT METHOD

This section explain how to attack the DRL-based scheduler for MU-MIMO without knowing the exact values of observations of victims. We begin by explaining our abstraction-based method to over-approximate the output of a DNN. Then, we formulate the network throughput degradation attack into a non-linear optimization problem, and solve it via stochastic gradient descent.

##### A. Compute DNN Output Bounds via Polytope

We opt for the polytope domain (e.g., DeepPoly [11]) as it is a precise and computationally efficient domain for general DNN verification problems. Note that the notation utilized in this section is distinct from that used in other sections and is applicable solely within the context of this particular section. The polytope abstract domain works by: (a) representing the input ranges of the DNN as polytopes, (b) applying transformation rules to the affine and non-linear units of DNN to obtain polytope regions representing output values of those units, and finally (c) converting the polytope results into output's lower and upper bounds. The resulting outputs are over-approximations of the actual outputs. This ensures the approximation remains conservative, meaning that the *actual outputs* are always contained within the predicted bounds.

Specifically, the abstraction *computes linear upper and lower bounds of the output of neural network  $N$  w.r.t input  $x \in \mathcal{X}$* , where  $\mathcal{X}$  is bounded input domain:

$$\underline{\mathbf{A}}x + \underline{\mathbf{b}} \leq N(x) \leq \overline{\mathbf{A}}x + \overline{\mathbf{b}}, \quad \forall x \in \mathcal{X}, \quad (8)$$

where the output of neural network  $N(x)$  is bounded by linear function of input  $x$ .  $\underline{\mathbf{A}}, \underline{\mathbf{b}}$  denote the coefficients for the lower bound hyper-plane, whereas  $\overline{\mathbf{b}}, \overline{\mathbf{A}}$  are those of the upper bound hyper-plane.

To get those of an  $L$ -layer feed-forward neural network  $N$ , it propagates bounds of  $N(x)$  as a linear function to the output of each layer, in a *backward* manner. Let  $h_j^{(i)}$  be the pre-activation of the  $j$ -th ReLU neuron in  $i$ -th layer, and  $g_j^{(i)}$  to denote the post-activation values. To compute the bounds for each layer, we start at the output layer  $N(x)$  (or  $h^{(L)}(x)$ ) with the following identity linear relationship:

$$h^{(L)}(x) \leq N(x) \leq h^{(L)}(x), \quad \forall x \in \mathcal{X}. \quad (9)$$

The next step then is to backward propagate from the identity linear relationship through the linear layer  $h^{(L)}(x) =$

$\mathbf{W}^{(L)}g^{(L-1)}(x)$  to get the linear bounds of  $N(x)$  w.r.t  $g^{(L-1)}(x)$  (for simplicity, we ignore biases):

$$\mathbf{W}^{(L)}g^{(L-1)}(x) \leq N(x) \leq \mathbf{W}^{(L)}g^{(L-1)}(x), \quad \forall x \in \mathcal{X}. \quad (10)$$

To get the linear bounds of  $N(x)$  w.r.t  $h^{(L-1)}(x)$ , we need to backward propagate through ReLU layer  $g^{(L-1)}(x) = \text{ReLU}(h^{(L-1)}(x))$ . Since it is nonlinear, we perform an approximation. Suppose that  $\mathbf{l}^{(L-1)} \leq h^{(L-1)}(x) \leq \mathbf{u}^{(L-1)}$  are intermediate pre-activation bounds of  $h^{(L-1)}(x)$ . If  $h^{(L-1)}(x)$  can only have positive ( $\mathbf{l}^{(L-1)} > 0$ ) or non-positive values ( $\mathbf{u}^{(L-1)} \leq 0$ ), then  $g^{(L-1)}(x) = h^{(L-1)}(x)$  or  $g^{(L-1)}(x) = 0$ , respectively.

When  $h^{(L-1)}(x)$  can have both positive and negative values ( $\mathbf{l}^{(L-1)} < 0 < \mathbf{u}^{(L-1)}$ ), we have:

$$\begin{aligned} g^{(L-1)}(x) &\geq \alpha^{(L-1)}h^{(L-1)}(x), \\ g^{(L-1)}(x) &\leq \frac{\mathbf{u}^{(L-1)}}{\mathbf{u}^{(L-1)} - \mathbf{l}^{(L-1)}}h^{(L-1)}(x) - \frac{\mathbf{u}^{(L-1)}\mathbf{l}^{(L-1)}}{\mathbf{u}^{(L-1)} - \mathbf{l}^{(L-1)}}, \end{aligned} \quad (11)$$

where the slope  $\alpha^{(L-1)}$  is a vector of 0 or 1 as defined in [11]. With these linear relaxations, we can get the linear equation of output  $N(x)$  w.r.t  $h^{(L-1)}(x)$ :

$$\begin{aligned} N(x) &\geq \mathbf{W}^{(L)}\underline{\mathbf{D}}_{\alpha}^{(L-1)}h^{(L-1)}(x) + \underline{\mathbf{b}}^{(L-1)}, \\ N(x) &\leq \mathbf{W}^{(L)}\overline{\mathbf{D}}_{\alpha}^{(L-1)}h^{(L-1)}(x) + \overline{\mathbf{b}}^{(L-1)}, \end{aligned} \quad (12)$$

where

$$\underline{\mathbf{D}}_{\alpha, (j,j)}^{(L-1)} = \begin{cases} \alpha_j^{(L-1)}, & \mathbf{W}_j^{(L)} \geq 0, \\ \frac{\mathbf{u}_j^{(L-1)}}{\mathbf{u}_j^{(L-1)} - \mathbf{l}_j^{(L-1)}}, & \mathbf{W}_j^{(L)} < 0, \end{cases} \quad (13)$$

$$\underline{\mathbf{b}}^{(L-1)} = \underline{\mathbf{b}}'^{(L-1)\top} \mathbf{W}^{(L)}, \quad (14)$$

$$\underline{\mathbf{b}}_j'^{(L-1)} = \begin{cases} 0, & \mathbf{W}_j^{(L)} \geq 0, \\ -\frac{\mathbf{u}_j^{(L-1)}\mathbf{l}_j^{(L-1)}}{\mathbf{u}_j^{(L-1)} - \mathbf{l}_j^{(L-1)}}, & \mathbf{W}_j^{(L)} < 0. \end{cases} \quad (15)$$

The diagonal matrices  $\underline{\mathbf{D}}_{\alpha}^{(L-1)}, \overline{\mathbf{D}}_{\alpha}^{(L-1)}$  and biases  $\underline{\mathbf{b}}^{(L-1)}, \overline{\mathbf{b}}^{(L-1)}$  reflect the linear relaxations and also consider the signs in  $\mathbf{W}^{(L)}$  to maintain the lower and upper bounds. The definitions for  $j$ -th diagonal element of  $\overline{\mathbf{D}}_{\alpha, (j,j)}^{(L-1)}$  and bias  $\overline{\mathbf{b}}^{(L-1)}$  are similar, with the conditions for checking the signs of  $\mathbf{W}_j^{(L)}$  swapped.

The abstraction to backward propagate these lower and upper bounds throughout the network, layer by layer (e.g.,  $h^{(L-2)}(x), g^{(L-2)}(x)$ , etc.), until reaching the input  $g^{(0)}(x) = x$ , getting the eventual bounding linear equations ( $\underline{\mathbf{A}}x + \underline{\mathbf{b}}$  and  $\overline{\mathbf{A}}x + \overline{\mathbf{b}}$ ) of  $N(x)$  in terms of input  $x$ .

##### B. Optimization Problem to Degrade Victim Throughput

The adversaries adjust their observations to cripple the throughput of the victims by minimizing the probability that victims are selected for data transmission, meaning the  $Q$ -value of any action  $a_t \in \mathcal{A}_{\text{vic}}$  containing a victim. Specifically, let  $o_{\text{adv}}$  represent the local observations of the adversaries and let  $\underline{o}_{\text{vic}}$  and  $\overline{o}_{\text{vic}}$  denote the lower and upper bounds of the local observations of the victims, respectively. With these inputs, the

adversarial cluster head computes the upper and lower bounds of the continuous proto actions ( $\underline{u}$  and  $\bar{u}$ ) using polytopes over-approximation as follows:

$$\underline{u}, \bar{u} = \text{POLYTOPE}(\pi(\cdot|o; \theta_\pi), \langle o_{\text{adv}}, \underline{o}_{\text{vic}} \rangle, \langle o_{\text{adv}}, \bar{o}_{\text{vic}} \rangle), \quad (16)$$

where  $\pi(\cdot|o; \theta_\pi)$  represents the trained actor models,  $\langle o_{\text{adv}}, \underline{o}_{\text{vic}} \rangle$  and  $\langle o_{\text{adv}}, \bar{o}_{\text{vic}} \rangle$  are the concatenations of adversarial inputs with the intervals of victim inputs. By leveraging the trained critic network  $Q(o, u; \theta_Q)$ , FGGM assesses the  $Q$ -value based on the inputs and proto actions. The final optimization problem for generating adversarial observations is as follows:

$$\underset{o_{\text{adv}}}{\text{minimize}} \quad \bar{q}, \quad (17)$$

such that

$$q, \bar{q} = \text{POLYTOPE}(Q(o, u; \theta_Q), \langle o_{\text{adv}}, \underline{o}_{\text{vic}}, u_i \rangle, \langle o_{\text{adv}}, \bar{o}_{\text{vic}}, u_i \rangle), \quad (18)$$

and

$$\mu_{\text{adv}} - \delta_{\text{adv}}\sigma_{\text{adv}} \leq o_{\text{adv}} \leq \mu_{\text{adv}} + \delta_{\text{adv}}\sigma_{\text{adv}}, \quad (19)$$

for all

$$\begin{cases} \underline{u} & \leq u_i \leq \bar{u}, \\ a_i & \in \mathcal{A}_{\text{vic}}, \end{cases} \quad (20)$$

where  $u_i$  is the proto action that corresponds to the discrete action  $a_i$ ,  $\mathcal{A}_{\text{vic}} \subset \mathcal{A}$  is the subset of actions that includes all actions containing victims, and  $[q, \bar{q}]$  in the estimated interval of  $Q$ -values. The values of the observation for adversaries should be clipped to fall within the desired range  $[\mu_{\text{adv}} - \delta_{\text{adv}}\sigma_{\text{adv}}, \mu_{\text{adv}} + \delta_{\text{adv}}\sigma_{\text{adv}}]$ , where  $\mu_{\text{adv}}$  and  $\sigma_{\text{adv}}$  are the mean and standard deviation of adversarial observations, and  $\delta_{\text{adv}}$  is a hyper-parameter to control the width of the search space. The objective is to minimize the upper bound of the  $Q$ -value for all possible actions containing victims.

Given that  $o_{\text{adv}}$  is differentiable, we can solve this problem using a standard gradient-based optimizer [24]. Since this optimization problem is non-linear, FGGM restarts many times to optimize  $o_{\text{adv}}$  from multiple initial values. Note that polytope abstraction ensures that the upper bound is always higher than the lower bound, minimizing only the upper bound  $Q$ -value leads to the reduction of the lower bound, and it is sufficient for the attack. Furthermore, the cluster head only needs to solve this problem once at the beginning of the attack period and the group of adversarial users can reuse the optimized adversarial observations for all time steps.

## V. EVALUATION AND DISCUSSION

We evaluate our adversarial attacks DRL-based MU-MIMO scheduler, and show that the proposed attack is effective in reducing network access probability and degrading throughput of victims. We focus our evaluation on the following research questions:

**RQ1** (§V-B): How does FGGM perform under various sizes of the search space for adversarial observations, and various sizes of bounds for observations of victims?

**RQ2** (§V-C): Can throughput degradation attack be performed more effectively if there are more adversarial users using FGGM?

**RQ3** (§V-D): What is the most significant consequence if the DRL-based scheduler is operating with 50% FGGM attackers?

### A. Experimental Design

1) *Benchmarking Environment*: To access our proposed attack, we created the target system based on a publicly available DRL algorithm for large-scale discrete action space [14], and trained this algorithm for the MU-MIMO scheduling problem [1]. The CSI values of all users were simulated using Quasi Deterministic Radio Channel Generator (QuaDRiGa) software [25]. We specifically examined a scenario where mobile users move at an average speed of 2.8 m/s with random directions. In this scenario, mobile users rebounded upon reaching the boundary, which is a circular area with a radius of 300 meters. Additionally, the environment utilized a 16-QAM modulation scheme, and the error vector magnitude of the received constellation is used to derive the signal-to-noise ratio. Further details on the hyper-parameters are presented in Tab. I.

Tab. I: Simulation parameters

| Parameter  | Values       |
|--|--------------|
| bandwidth  | 20 MHz       |
| carrier frequency                                | 3.6 MHz      |
| slot duration                                    | 1ms          |
| number of time slots                             | 500          |
| number of users ( $L$ )                          | {8, 16}      |
| number of antennas ( $M$ )                       | {4, 16}      |
| maximum users per time slot ( $\bar{N}$ )        | {4, 4}       |
| proportional fairness coefficient $\beta$        | 0.5          |
| number of dimension of proto action $D$          | {3, 8}       |
| number of nearest neighbor $K$                   | {20, 20}     |
| number of hidden units in Actor                  | 128          |
| number of hidden units in Critic                 | 256          |
| number of hidden layers in Actor and Critic      | 2            |
| activation function in Actor and Critic          | ReLU         |
| number of adversarial users ( $L_{\text{adv}}$ ) | up to {4, 8} |
| number of FGGM/SPGD iterations                   | 300          |
| number of FGGM/SPGD restarts                     | 10           |
| number of SPGD samples                           | 100          |

2) *Baselines*: The performance of our proposed attack FGGM is compared with that of conventional schedulers and other potential schemes for generating adversarial observations. Conventional schedulers include policies such as Random, OptPF, optimal max rate (OptMR), optimal proportional fairness with user grouping (OptPFUG), and SAC. In each time slot  $t$ , the Random policy randomly selects one action from the action set  $\mathcal{A}$ . OptMR and OptPF policies exhaustively evaluate the action set  $\mathcal{A}$  to determine the action that yields the highest data rate or proportional fairness score (Eq. 6). However, OptMR and OptPF are not scalable for more users as their computational complexities are  $\mathcal{O}(2^L)$ , where  $L$  is the number of total users sharing the same resource block. OptPFUG reduces the complexity by grouping users with channel correlation less than 0.5 in the same group and selecting the group providing the highest proportional fairness score. Similarly, SAC is a scalable method for MU-MIMO

scheduling, as it takes a polynomial time to infer the set of users from the trained actor and critic networks (§II-C).

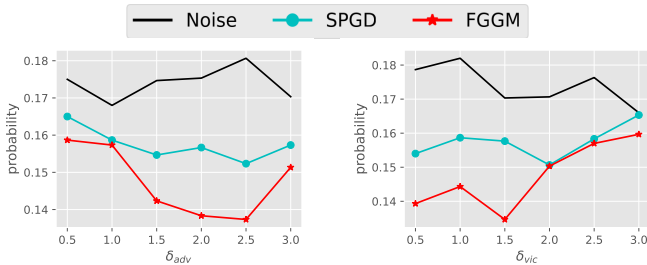
Three adversarial attack schemes are considered: (1) Noise, (2) sampling-based projected gradient descent (SPGD), and (3) our proposed attack FGGM. Noise generates random CSI at each time slot  $t$  for adversarial users to disrupt the SAC scheduler, regardless of the observations of the victims, and it represents the class of black-box attacks. SPGD is our adapted version of the origin PGD [26] to perform grey-box attack. It randomly generates samples of CSIs within the estimated bounds of the observations of victims and then solves the same problem in §IV-B for the generated set of samples. To ensure fairness in our comparison, SPGD and FGGM have the same number of iterations and number of restarts (Tab. I).

3) *Evaluation metrics*: We compare the performance of MU-MIMO schedulers and attack schemes via four main metrics; namely, proportional fairness, Jain fairness index (JFI), the selection probability of victims, and average data rate of victims. To compute these metrics, we run the simulator for 500 time slots using the same CSI trace from QuaDRiGa [1, 25], and record the set of selected users as well as each of their instantaneous transmission rates. The proportional fairness per each time slot is calculated according to Eq. 6, and the Jain fairness index at each time slot  $t$  is defined as:

$$JFI^t = \frac{(\sum_{l=1}^L R_l^t)^2}{L \sum_{l=1}^L (R_l^t)^2}, \quad (21)$$

where  $R_l^t$  is the long-term average rate in Eq. 5.

### B. RQ1: Performance under Varying Search Space



(a) Varying adversary bounds (b) Varying victim bounds

Fig. 3: The average selection probability of victims when attacker using different attacking schemes to create adversarial CSIs.  $L = 8, M = 4$ , and  $\bar{N} = 4$ .  $\delta_{vic}$  and  $\delta_{adv} \in \{0.5, 1.0, 1.5, 2.0, 2.5, 3.0\}$ . Lower is better.

The performances of three attacking schemes are analyzed in Fig. 3 as the search space sizes vary for observations of adversaries  $\delta_{adv}$  and estimate errors for observations of victims  $\delta_{vic}$ . Since  $\delta_{adv}$  is measured in terms of standard deviations that adversarial observations can deviate from the average, the searching domain for adversarial users is defined as  $\mu_{adv} \pm \delta_{adv} \sigma_{adv}$ , where  $\mu_{adv}$  and  $\sigma_{adv}$  represent the average and standard deviation of the observations of adversarial users,

respectively. Similarly,  $\delta_{vic}$  describes the estimated range within which the observations of victims belong, given by  $\mu_{vic} \pm \delta_{vic} \sigma_{vic}$ .

A grid search is conducted on  $6^2$  different configurations. Fig. 3a illustrates the victim selection probabilities for each value of  $\delta_{adv}$  averaged across different values of  $\delta_{vic}$ . Likewise, Fig. 3b demonstrates the victim selection probabilities for each value of  $\delta_{vic}$  averaged across different values of  $\delta_{adv}$ . Overall, both figures show that FGGM facilitated a lower victim selection probabilities than the comparing schemes in all configurations. Additionally, both grey-box attacks SPGD and FGGM provided strictly better adversarial inputs than Noise.

We would like to draw readers' attention to the plot for the varying adversarial bounds in Fig. 3a. The victim selection probabilities of FGGM gradually decreased from the starting point, bottomed out at  $\delta_{adv} = 2.5$  before increasing again towards the end. As anticipated, our experiments show that FGGM would not be able to search for good adversarial observations when the search space was small ( $\delta_{adv} \leq 1.0$ ) as there does not exist any satisfied solution. FGGM struggled at  $\delta_{adv} = 3$  because the stochastic gradient descent algorithm cannot navigate this large search space. At the medium search space configuration such as  $\delta_{adv} = 2.0$ , FGGM achieved a low victim access probability at 13.8%, while SPGD and Noise reached 15.7% and 17.5%, respectively.

Regarding the ablation study for victim bounds in Fig. 3b., FGGM only exceeded SPGD with a wide margin when  $\delta_{vic} \leq 1.5$ . This is consistent with the literature on DNN verification, as wider input bounds lead to huge errors in estimating the output bounds, which reduce the effectiveness of DNN verification.

**RQ1 Findings:** FGGM produced a strictly lower victim access probability than SPGD and Noise. Under the best parameter, FGGM was 21.1% better than black-box attack and 12.1% better than SPGD in terms of victim access probability.

### C. RQ2: Performance under Varying Number of Attackers



(a) Selection probability (b) Transmission rate

Fig. 4: The minimum probability and transmission rate of victims as the number of attackers increased from 1 to 8.  $L = 16, M = 16$ , and  $\bar{N} = 4$ .

From now on, we select the best parameter for the following experiments:  $\delta_{adv} = 2.0$  and  $\delta_{vic} = 1.5$ .

Fig. 4 presents an ablation study on the impact of the number of attackers on victims’ performances. In general, both gradient-based grey-box attack methods showed significant improvements compared to `Noise`, and our proposed `FGGM` method surpassed `SPGD` in almost all searched numbers of attackers. In the presence of a grey-box attack, there is a correlation between the number of attackers and the reduction in selection probabilities and transmission rates of victims. In contrast, increasing number of attackers in `Noise` did not proportionally decrease service quality. Note that, even with only one adversarial user, the `FGGM` slashed the transmission rate of victims by 9.5% more than those of `Noise` scheme.

In the most favorable scenario where adversarial users occupied half of the considered resource block, the worst transmission rate of victims reduced to half of that of the `Noise` attacking scheme. The rationale behind this trend is that higher number of attackers means smaller number of unknown inputs, leading to a smaller input domain. It enables `FGGM` to estimate the upper bound of  $Q$ -value more precisely, further diminishing the throughput and access probability of victims.

#### D. RQ3: Impact under 50% Attack

At this point, we discuss the impact of our attack to DRL-based MU-MIMO system under the best parameters obtained from the previous ablation studies. Fig. 5 shows the disruption of the attack in our small setting of 8 users per resource block. We observed that without disruption, the `SAC` scheduler provided nearly similar performance to `OptPF` scheduler in terms of worst victim throughput, proportional fairness, and Jain fairness index. This suggests that our DRL-based scheduler has been well trained. However, the `Noise` attacker degraded the performance of `SAC` back to the same level as `Random`. The main reason is that our standard `SAC` algorithm for large-scale discrete action problems lacks adversarial training [27], and it also highlights the emergent need for robust DRL training. As shown in Fig. 5a, `SPGD` degrades `SAC` by reducing the data rate from 88.5 MB/s to just under 52.3 MB/s, while `FGGM`, with the formal verification technique, further halves the throughput of the victim, at an impressive 70%, which is about 26.6 MB/s.

In Fig. 6, as the number of users and attackers doubled, the pattern remained the same. For instance, the `FGGM` significantly reduced the worst victim delivered data rate and Jain fairness index. `SPGD` showed improvement from `Noise`, but `FGGM` was still stand out as the best attacking method. It demonstrates that minimizing the upper bound of the output  $Q$ -value is more effective than sampling a limited number of examples for a `PGD` attack. Fig. 6a indicates that `FGGM` still reduced the victim’s throughput by 46% in compared with the original DRL-based MU-MIMO scheduler. From the box plots in Fig. 6b and Fig. 6c, we observe that `FGGM` attack notably reduced Jain fairness distribution of `SAC` but did not have any impact on proportional fairness distribution. This implies that training the DRL-based to maximize multiple fairness

metrics may improve the robustness of the DRL agent against adversarial attacks.

**RQ3 Findings:** Under 50% attack, `FGGM` reduce victim data rate from about 46% to 70%. In resource block with 8 users, data rates of DRL-based scheduler were crippled from 88.5 MB/s to merely 26.6 MB/s.

## VI. RELATED WORKS

We review several algorithms that are based on DNN for solving resource allocation problems in MU-MIMO, with the emphasis on their potential unsanitized inputs. We then discuss related works on exploiting of these algorithms.

### A. DNN for Resource Allocation in MU-MIMO

The multi-user scheduling problem presents a significant challenge in resource allocation due to its computational complexity. To reduce the complexity of traditional optimization-oriented methods, many papers advocate DNN-based wireless resource allocation algorithms for different problems. Recently, DRL has been introduced as a solution to approximate the optimal allocation strategy [7]. For instance, in [28], the Levenberg-Marquardt algorithm is utilized to optimize a fully connected neural network that maps the channel state information (CSI) to the user set to maximize the sum rate. Alternatively, [29] proposes a method where users directly report their CSI to the base station (base station), which trains a DRL model to select a subset of users for transmission to maximize the sum rate. Moreover, in [30], a real-time deep deterministic policy gradient (DDPG) model is developed with CSI as the main input for user selection during transmission. Similarly, [31] introduces a `SAC` network that utilized CSI for user selection. Conversely, in [32], previous achievable rates and channel correlation matrices derived from CSI is used to determine both the user set and their channel precoding strategy. Additionally, [33] incorporates channel quality index, data amount, and data type as the state variables in the selection algorithm across multiple layers. Lastly, [1] implements a vanilla `SMART` approach where CSI served as input for a DNN actor, showcasing one of the most effective methods for multi-user scheduling.

In summary, the input of recently proposes DNN-based resource allocation algorithms in massive MIMO included the CSI, large scale fading coefficient, spectral noise, SINR, or transmission rate. Note that they can be modified by a group of adversarial users, and so the DNN output could be manipulated to achieve malicious goals. The next section provides an overview of existing attacks to the input of DNN-based resource allocation algorithms.

### B. Attacking Algorithms for Resource Allocation in MU-MIMO

Recent works proposed attacks on DNN-based wireless resource allocation algorithms such as power allocation, resource slicing, and multi-user scheduling.

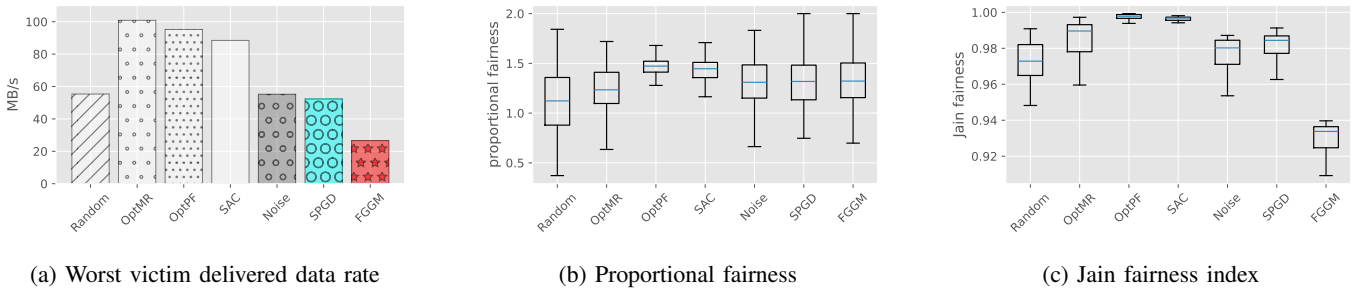


Fig. 5: Performance of all schedulers and attacking schemes in networks configuration with  $L = 8$ ,  $M = 4$ ,  $\bar{N} = 4$ , and  $L_{adv} = 4$

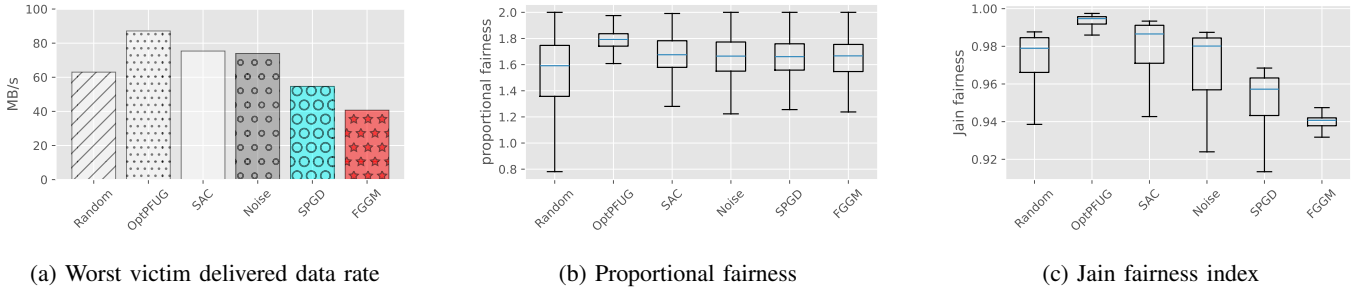


Fig. 6: Performance of all schedulers and attacking schemes in networks configuration with  $L = 16$ ,  $M = 16$ ,  $\bar{N} = 4$ , and  $L_{adv} = 8$

In [10], the authors conduct a white-box attack on a DNN-based regression model that learned a mapping from users' geographical positions to the optimal power allocation, obtained by solving the problem using traditional optimization tools. The threat model involves attackers overwriting the positioning information of nearby users so to manipulate the network input using fast gradient sign method (FGSM) [8, 34], PGD [26], and momentum iterative fast gradient sign method (MI-FGSM) [35]. Similarly, other works [36, 37] proposes gradient-based white-box attacks on the full input of the DNN, while maintaining the assumption of knowing the exact location of all users, which is impractical. To address this issue, [38] proposes a black-box attack based on universal adversarial perturbation (UAP) [39]. However, the evaluation reveals that the black-box attack lacks of stealthiness as it is effective only with large perturbation magnitudes. Additionally, previous works allow the adversary to apply adversarial perturbations to the full input of the DNN.

In [40], a resource slicing attack based on Q-learning was carried out. To reduce the Q-learning resource slicing agent's reward, they suggests to train another Q-learning agent as an attacker. This Q-learning-based attacker selects the resource block and sent a jamming signal within a limited energy budget. Subsequently, [41] introduces a multi-agent deep reinforcement learning (MADRL) resource slicing system, where each agent represented a base station in a multi-cell architecture. These agents are trained using centralized training decentralized execution to map user requests to available channel resources, maximizing the system's throughput. An

attacker is also trained to select resources to jam in order to minimize the system's global reward. Note that training an attacker is computationally intensive and may not effectively exploit vulnerabilities in trained resource slicing agents.

In [9], a black-box heuristic attack is proposed to target the heuristic selection of users in multi-user scheduling in massive MIMO networks. The advantage of this work is that only a few attackers need to manipulate the CSI in the networks. However, they assumes that attackers could passively listen and accurately determine the current CSI of normal users, without investigating how to attack the DRL-based multi-user scheduling system.

In conclusion, our work differs from existing literature by assume that adversaries only manipulate a small fraction of the attacker's input to DRL models, without the knowledge of local observations of normal users.

## CONCLUSION

In this paper, we present FGGM, a technique designed to generate adversarial observations that compromise the functionality of DRL-based resource allocation algorithms. Unlike other previous attacking schemes, FGGM only controls a part of the observations, and does not require the exact knowledge of the other uncontrollable parts. Experimental results on DRL-based scheduler for massive MU-MIMO networks show that adversarial observations generated by FGGM effectively reduced the allocated resources to victims without the exact knowledge of their local observations. By constructing an objective function based on output bounds, the adversarial

inputs have been optimized using stochastic gradient descent to achieve specific goals, such as minimizing the likelihood of the victim being selected for transmission.

#### REFERENCES

- [1] Qing An et al. “A Deep Reinforcement Learning-Based Resource Scheduler for Massive MIMO Networks”. In: *IEEE Transactions on Machine Learning in Communications and Networking* (2023).
- [2] Thomas L Marzetta, Erik G Larsson, and Hong Yang. *Fundamentals of Massive MIMO*. Cambridge University Press, 2016.
- [3] R Mounika, Abhinav Kumar, Kiran Kuchi, et al. “Downlink Resource Allocation for 5G-NR Massive MIMO Systems”. In: *2021 National Conference on Communications (NCC)*. IEEE. 2021, pp. 1–6.
- [4] Vincent KN Lau. “Proportional fair space-time scheduling for wireless communications”. In: *IEEE Transactions on Communications* 53.8 (2005), pp. 1353–1360.
- [5] Tien Thanh Le, Yusheng Ji, and John CS Lui. “TinyQMIX: Distributed access control for mMTC via multi-agent reinforcement learning”. In: *2022 IEEE 96th Vehicular Technology Conference (VTC2022-Fall)*. IEEE. 2022, pp. 1–6.
- [6] Tien Thanh Le, Yusheng Ji, and John C. S. Lui. “MFTTS: A Mean-Field Transfer Thompson Sampling Approach for Distributed Power Allocation in Unsourced Multiple Access”. In: *IEEE Transactions on Mobile Computing* 23.12 (2024), pp. 11312–11325. DOI: 10.1109/TMC.2024.3399876.
- [7] Irwan Bello et al. “Neural Combinatorial Optimization with Reinforcement Learning”. In: *arXiv preprint arXiv:1611.09940* (2016).
- [8] Sandy Huang et al. “Adversarial attacks on neural network policies”. In: *arXiv preprint arXiv:1702.02284* (2017).
- [9] Tao Hou et al. “MUSTER: Subverting user selection in MU-MIMO networks”. In: *IEEE INFOCOM 2022-IEEE Conference on Computer Communications*. IEEE. 2022, pp. 140–149.
- [10] BR Manoj, Meysam Sadeghi, and Erik G Larsson. “Adversarial attacks on deep learning based power allocation in a massive MIMO network”. In: *ICC 2021-IEEE International Conference on Communications*. IEEE. 2021, pp. 1–6.
- [11] Gagandeep Singh et al. “An abstract domain for certifying neural networks”. In: *Proceedings of the ACM on Programming Languages* 3.POPL (2019), pp. 1–30.
- [12] Changliu Liu et al. “Algorithms for verifying deep neural networks”. In: *Foundations and Trends® in Optimization* 4.3-4 (2021), pp. 244–404.
- [13] Hai Duong et al. “A DPLL(t) Framework for Verifying Deep Neural Networks”. In: *arXiv preprint arXiv:2307.10266* (2023).
- [14] Gabriel Dulac-Arnold et al. “Deep Reinforcement Learning in Large Discrete Action Spaces”. In: *arXiv preprint arXiv:1512.07679* (2015).
- [15] Tuomas Haarnoja et al. “Soft Actor-Critic Algorithms and Applications”. In: *arXiv preprint arXiv:1812.05905* (2018).
- [16] Guy Katz et al. “Reluplex: a calculus for reasoning about deep neural networks”. In: *Formal Methods in System Design* 60.1 (2022), pp. 87–116.
- [17] Hai Duong et al. “Harnessing Neuron Stability to Improve DNN Verification”. In: *Proc. ACM Softw. Eng.* 1.FSE (July 2024). DOI: 10.1145/3643765. URL: <https://doi.org/10.1145/3643765>.
- [18] Hai Duong, ThanhVu Nguyen, and Matthew B Dwyer. “NeuralSAT: A High-Performance Verification Tool for Deep Neural Networks”. In: *International Conference on Computer Aided Verification*. Springer. 2025, pp. 409–423.
- [19] Hai Duong and ThanhVu Nguyen. “Neuralsat: Scaling constraint solving for dnn verification (competition contribution)”. In: *International Symposium on AI Verification*. Springer. 2025, pp. 253–259.
- [20] Hai Duong et al. “Compositional neural network verification via assume-guarantee reasoning”. In: *The Thirty-ninth Annual Conference on Neural Information Processing Systems*. 2025.
- [21] Hai Duong et al. “Verifying Structural Robustness of Deep Neural Network”. In: *Proceedings of the ACM on Software Engineering* 3.FSE (2026), to appear.
- [22] Dong Xu et al. “Training for Verification: Increasing Neuron Stability to Scale DNN Verification”. In: *Tools and Algorithms for the Construction and Analysis of Systems*. Ed. by Bernd Finkbeiner and Laura Kovács. Cham: Springer Nature Switzerland, 2024, pp. 24–44. ISBN: 978-3-031-57256-2.
- [23] Horia Mania, Aurelia Guy, and Benjamin Recht. “Simple random search provides a competitive approach to reinforcement learning”. In: *arXiv preprint arXiv:1803.07055* (2018).
- [24] Diederik P Kingma and Jimmy Ba. “Adam: A method for stochastic optimization”. In: *arXiv preprint arXiv:1412.6980* (2014).
- [25] Stephan Jaeckel et al. “QuaDRiGa: A 3-D multi-cell channel model with time evolution for enabling virtual field trials”. In: *IEEE transactions on antennas and propagation* 62.6 (2014), pp. 3242–3256.
- [26] Aleksander Madry et al. “Towards deep learning models resistant to adversarial attacks”. In: *arXiv preprint arXiv:1706.06083* (2017).
- [27] Tuomas Oikarinen et al. “Robust deep reinforcement learning through adversarial loss”. In: *Advances in Neural Information Processing Systems* 34 (2021), pp. 26156–26167.
- [28] Junchao Shi et al. “Machine Learning Assisted User-Scheduling Method for Massive MIMO System”. In: *2018 10th International Conference on Wireless Communications and Signal Processing (WCSP)*. IEEE. 2018, pp. 1–6.
- [29] Gaojing Bu and Jing Jiang. “Reinforcement learning-based user scheduling and resource allocation for massive MU-MIMO system”. In: *2019 IEEE/CIC International Conference on Communications in China (ICCC)*. IEEE. 2019, pp. 641–646.
- [30] Xiaojun Guo et al. “A novel user selection massive MIMO scheduling algorithm via real time DDPG”. In: *GLOBECOM 2020-2020 IEEE Global Communications Conference*. IEEE. 2020, pp. 1–6.
- [31] Liang Chen et al. “Deep reinforcement learning for resource allocation in massive MIMO”. In: *2021 29th European Signal Processing Conference (EUSIPCO)*. IEEE. 2021, pp. 1611–1615.
- [32] Hongchao Chen et al. “Joint user scheduling and transmit precoder selection based on DDPG for uplink multi-user MIMO systems”. In: *2021 IEEE 94th Vehicular Technology Conference (VTC2021-Fall)*. IEEE. 2021, pp. 1–5.
- [33] Chih-Wei Huang et al. “A DRL-based automated algorithm selection framework for cross-layer QoS-aware scheduling and antenna allocation in massive MIMO systems”. In: *IEEE Access* 11 (2023), pp. 13243–13256.
- [34] Ian J Goodfellow, Jonathon Shlens, and Christian Szegedy. “Explaining and harnessing adversarial examples”. In: *arXiv preprint arXiv:1412.6572* (2014).
- [35] Yinpeng Dong et al. “Boosting adversarial attacks with momentum”. In: *Proceedings of the IEEE conference on computer vision and pattern recognition*. 2018, pp. 9185–9193.
- [36] Qing Liu et al. “Adversarial attack on DL-based massive MIMO CSI feedback”. In: *Journal of Communications and Networks* 22.3 (2020), pp. 230–235.
- [37] Brian Kim et al. “Adversarial attacks against deep learning based power control in wireless communications”. In: *2021*

*IEEE Globecom Workshops (GC Wkshps)*. IEEE. 2021, pp. 1–6.

- [38] Pablo Millán Santos et al. “Universal adversarial attacks on neural networks for power allocation in a massive MIMO system”. In: *IEEE Wireless Communications Letters* 11.1 (2021), pp. 67–71.
- [39] Seyed-Mohsen Moosavi-Dezfooli et al. “Universal adversarial perturbations”. In: *Proceedings of the IEEE conference on computer vision and pattern recognition*. 2017, pp. 1765–1773.
- [40] Yi Shi et al. “How to Attack and Defend NextG Radio Access Network Slicing with Reinforcement Learning”. In: *IEEE Open Journal of Vehicular Technology* 4 (2022), pp. 181–192.
- [41] Feng Wang, M Cenk Gursoy, and Senem Velipasalar. “Robust Network Slicing: Multi-Agent Policies, Adversarial Attacks, and Defensive Strategies”. In: *IEEE Transactions on Machine Learning in Communications and Networking* (2023).